Proceedings 10th NUMGE 2023
10th European Conference on Numerical Methods in Geotechnical Engineering
Zdravkovic L, Kontoe S, Taborda DMG, Tsiampousi A (eds)

https://doi.org/10.53243/NUMGE2023-345

Numerical modelling of stiffness and damping evolution of offshore monopile foundations under lateral cyclic loading

I.O. Aghedo[1], T.S. Charlton[1], M. Rouainia[1]

[1]*School of Engineering, Newcastle University, Newcastle Upon Tyne, UK*

ABSTRACT: Numerical modelling is fundamental to validating and improving monopile design approaches and the soil constitutive model is a key component. Here, a three-dimensional finite element model of a large diameter monopile is developed based on an advanced soil constitutive model for clay, which has been calibrated with experimental results. The kinematic hardening soil model can capture the accumulation of plastic strains, build-up of pore water pressure, and degradation of shear stiffness and initial structure that characterise the response of natural clay. The monopile is subjected to one-way lateral cyclic loading and the effect of loading intensity and overconsolidation ratio on the cyclic secant stiffness and damping ratio are investigated. The monopile showed ratcheting, where rotation accumulates with increasing numbers of load cycles, and the formation of hysteresis loops in each cycle. In normally consolidated clay, the stiffness decreased, and the damping ratio increased due to excess pore water pressures causing a softer soil response. In contrast, in overconsolidated clay, the stiffness showed an increase because negative excess pressures were generated in the soil deposit. The results demonstrate the importance of pore pressure generation in controlling monopile response and provide some guidance in the engineering design of monopiles in clay deposits.

Keywords: Monopile; Numerical modelling; Damping; Stiffness; Clay

1 INTRODUCTION

Offshore wind has advanced rapidly over the past decade and is essential to the UK's decarbonisation agenda, which aims to achieve net zero carbon emissions by 2050 (HM Government, 2019). About 80% of offshore wind turbines (OWTs) in Europe are currently supported on monopile foundation systems, which are open-ended steel tubes with a typical diameter of >3 m (Wind Europe, 2020).

The diameter of monopile foundations and wind turbines will increase in future installations due to the generation of greater power output from the environmental forces of wind and waves in deeper waters. Therefore, the main challenge for offshore wind developers is to reduce the cost of offshore wind farms while utilizing larger turbines in deeper waters. One step toward achieving this goal is improved design and optimisation of the foundation structure. According to inventories, the cost of the foundation accounts for about 30% of the overall cost of an offshore wind farm (Malekjafarian et al., 2021). Therefore, a better understanding of monopile performance, leading to design optimisation, is key to bringing down the levelised cost of energy (LCOE).

A monopile foundation system is subjected to consistent lateral load cycles from wind and waves over its lifetime (around 25-30 years). The design must account for the ultimate limit state (ULS), serviceability limit state (SLS), and fatigue limit state (FLS). Recent Joint industry research, e.g PISA project (Byrne et al., 2020), has made significant progress in predicting the ultimate load conditions of the monopile. However, the cyclic behaviour of laterally loaded monopiles needs further study.

In recent years, several experimental (Kong et al., 2022; Kou et al., 2022; Lai et al., 2020, 2022) and numerical (Charlton and Rouainia, 2021; Cheng et al., 2021; Duque et al., 2021; Xie and Lopez-Querol, 2021) studies have been performed to understand the behaviour of monopiles under cyclic loading in clay. However, there is still a lack of proper understanding of the evolution of damping and stiffness over time. The foundation damping plays an important role in the design process and is highly dependent on soil damping (GL, 2005), which is derived from the hysteretic response of the soil. For example, if the monopile experiences more damping, the stress amplitudes during cyclic loading will be lower, and thus the accumulation of fatigue damage will be smaller, potentially increasing the structure's lifetime.

In addition, recent research by Lai et al. (2020) involving centrifuge testing of a monopile subjected to a series of cyclic remoulding and reconsolidation episodes revealed that pile-soil stiffness and strength decrease during cyclic remoulding and partially or entirely recover during the reconsolidation stage. These findings highlight the importance of considering the stress history of clay when evaluating pile-soil stiffness. Considering the effect long-term cyclic loading may have on the foundation response, which determines the primary mode of vibration of the structure, it is crucial to evaluate any changes in this stiffness over time for an accurate prediction of the fatigue life.

To address the above limitations, this paper focuses on numerical modelling of a large diameter monopile in a cohesive soil (London clay). The cyclic behavior of the laterally-loaded monopile will be investigated in terms of (i) accumulation of permanent deformations, (ii) stiffness of the foundation, and (iii) foundation damping, which are all critical factors in the serviceability and fatigue designs of the foundation. Both overconsolidated and normally consolidated clay deposits are considered.

2 CONSTITUTIVE MODEL

When clays are subjected to undrained cyclic loading, complex phenomena such as the build-up of plastic strains, the increase in pore water pressure, and the deterioration of the initial structure and shear stiffness are evident. Implementing a constitutive model that can account for these effects is therefore crucial to capturing realistic foundation performance. The constitutive soil model formulated by Rouainia-Muir Wood (RMW) (Rouainia & Muir Wood, 2000), a multi-surface effective stress model based on the critical state framework, has been implemented in this research. The RMW model extends the conventional Modified Cam Clay (MCC) model (Roscoe and Burland, 1968) by the addition of a structure surface which represents an initial amount of structure that controls the process of destructuration and progressively collapses to the reference MCC surface due to the development of plastic strains. The degradation of stiffness is captured through a bounding surface relationship, with stiffness dependent on the distance between the bubble and structure surface. Refer to Rouainia and Muir Wood (2000) for more details on the formulation and implementation of the RMW. The shear stiffness, G, is described using a non-linear elastic formulation by Viggiani and Atkinson (1995):

$$\frac{G}{P_r'} = A_g \left(\frac{p'}{P_r'}\right)^{n_g} R_0{}^{m_g} \quad (1)$$

where A_g, n_g and m_g are dimensionless stiffness parameters, $R_0 = 2P_C/p'$ is the isotropic consolidation ratio, with P_C the centre of the reference surface, p' is the mean effective stress with a reference value P_r' of 1kPa. The RMW parameters were calibrated to triaxial test results on London clay, a stiff overconsolidated clay with high peak strength (Gasparre et al., 2007; Gasparre and Coop, 2008). The calibration was carried out by Gonzàlez et al (2012) for analysis of tunnel excavation in London clay. The intrinsic parameters of the clay: modified compression index λ^{*}, modified swelling index κ^{*}, and critical state stress ratio M, were obtained from extensive laboratory characterisation presented by Gasparre (2005). The clay has a bulk unit weight of 19kN/m^3 and a critical friction angle of 22°. The overconsolidation ratio was set to 4.5 for overconsolidated clay and 1.0 for the normally consolidated clay. The calibrated parameters are presented in Table 1

Table 1. Calibrated RMW parameters for London Clay

Material property	Value
Slope of normal compression line, λ^*	0.0965
Slope of swelling line, κ^*	0.0459
Poisson's ratio, v	0.3
Critical state stress ratio, M	0.85
Ratio of size of bubble and reference surface, R	0.016
Stiffness interpolation parameter, B	4.0
Stiffness interpolation exponent, ψ	6.0
Initial degree of structure, r_0	2.5
Destructuration strain parameter, A	0.75
Destructuration parameter, k	1.0
Non-dimensional stiffness parameter, A_g	430
Non-dimensional stiffness parameter, n_g	0.87
Non-dimensional stiffness parameter, m_g	0.28

3 FINITE ELEMENT MODEL

The effect of lateral cyclic loading on a monopile in London clay is investigated using a 3D finite element (FE) model (Plaxis, 2022). The monopile is modelled as a rigid plate with an outer diameter of 3.8m, wall thickness of 56mm and embedded depth of 20m. Dynamic sinusoidal forces with a frequency of 0.2Hz, which falls within the range of expected ocean wave frequencies for the North Sea (Hasselman et al., 1973), are applied to the monopile top, 30m above the mudline. The FE mesh consists of 5520 10-node tetrahedral elements, as shown in Figure 1. Due to symmetry and to reduce computational time, only half of the pile is modelled with viscous lateral boundaries applied to absorb outgoing energy in dynamic analyses, except along the line of symmetry. Installation effects are ignored, with the monopile wished-in-place at the beginning of each simulation. The interaction between the pile and the soil is modelled through interface elements with a reduced strength of $\varphi = 14°$. A Young's modulus of $E = 210$ GPa and Poisson's ratio $v = 0.3$ are assigned to the steel monopile. Undrained conditions are applied.

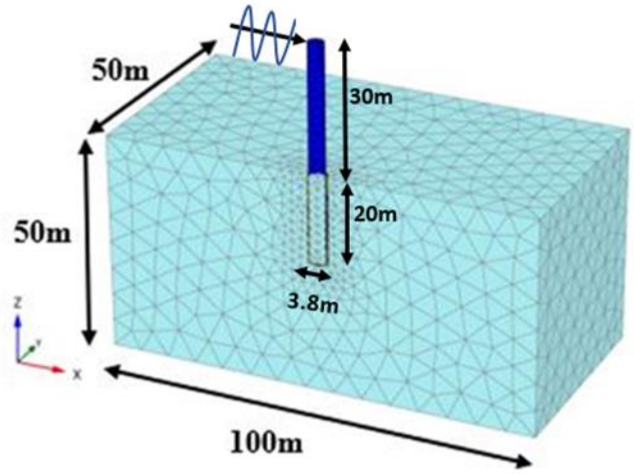

Figure 1. 3D finite element mesh

Three load cases of one-way cycles are considered to assess performance at both the FLS (ζ_b = 0.18, 0.25) and SLS (ζ_b = 0.47) (LeBlanc et al., 2010) where:

$$\zeta_b = \frac{F_{max}}{F_R} \tag{2}$$

F_R is the static capacity (5.44MN) and F_{max} the maximum load applied in each cycle.

4 RESULTS AND DISCUSSION

The pile response to lateral cyclic loading is assessed in terms of (a) accumulated rotation, (b) secant stiffness, and (c) damping ratio. Both overconsolidated and normally consolidated clay are analysed.

4.1 Overconsolidated clay

4.1.1 Accumulated rotation

Figure 2 shows the moment-rotation *(M-θ)* curve at the mudline under various load intensities of one-way cycles $\zeta_b = \{0.18, 0.25, 0.47\}$. Up to 100 cycles are applied to the monopile. The *M-θ* curve demonstrates that significant accumulated pile rotation occurs under cyclic loading, with the cyclic loading intensity gradually increasing from 0.18 to 0.47. At each loading intensity, the *M-θ* curve exhibits a significant nonlinear hysteretic response due to energy dissipation in each load cycle. The predicted hysteresis loops reveal the monopile foundation's nonlinear response in clays. The hysteresis loops do not close, which means that as loading-unloading cycles continue, the monopile experiences ratcheting.

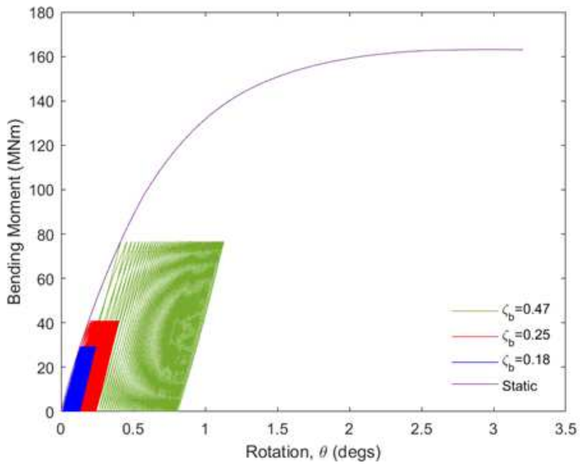

Figure 2. Bending moment-rotation at the mudline for different loading magnitudes (OCR=4.5)

4.1.2 Secant stiffness

The evolution of secant stiffness with cycle number for an overconsolidated clay is depicted in Figure 3. At each loading intensity, the secant stiffness increases as with increasing number of cycles. The rate of increase in secant stiffness is rapid during the first 20 cycles but attenuates as more load cycles are applied. This phenomenon could be explained by the generation of negative excess pore pressures around the monopile, which results in a stiffer response. The secant stiffness decreases with increasing load magnitudes (ζ_b) owing to an increase in the development of plastic strains around the monopile. The stiffer pile response could have a negative effect on the OWT by shifting the natural frequency of the OWT, towards the 3P blade passing frequency which could result in damaging resonance effects.

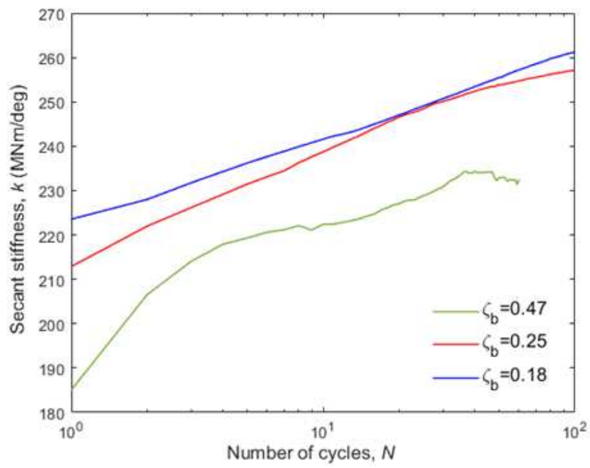

Figure 3. 100 one-way cyclic test results: Evolution of secant stiffness with cycle number (OCR=4.5)

4.1.3 Damping ratio

Soil hysteretic damping is commonly studied using the damping ratio (Abadie et al., 2019) which can be calculated by:

$$D_a = \frac{1}{4\pi} \frac{A_{hys}}{A_{el}} \quad (3)$$

where D_a is the damping ratio, A_{hys} is the dissipated energy during a cycle and A_{el} is the stored elastic energy. Figure 4 shows the evolution of damping with cycle numbers for an overconsolidated clay. The damping ratio is higher at greater load intensities due to the development of larger stress amplitudes. At each loading intensity, the damping ratio decreases with increasing load cycles. The damping exhibits two trends: a sharp decrease during the first N = 10 cycles followed by a gradual decrease as N increases to 100 cycles. Again, this phenomenon could be explained by the generation of negative pore water pressures which stiffens the pile response. These findings are consistent with those reported by Beuckelaers (2017), who also observed a decrease in damping ratio with increasing load cycles for monopiles in Cowden till, an overconsolidated clay.

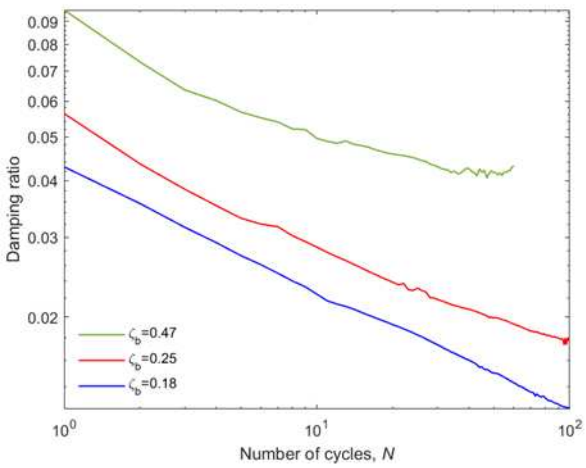

Figure 4. 100 one-way cyclic test results: Evolution of damping with cycle numbers (OCR=4.5)

4.1.4 Pore water pressure

Figure 5 shows the pore water pressure around the monopile in overconsolidated clay after 100 load cycles at ζ_b = 0.25. As a result of the overconsolidated state of the clay, a zone of negative excess pore pressure in the form of a wedge-shape develops on both sides of the monopile, thereby increasing the effective stress and consequently causing a stiffer response of the monopile which leads to an increase in secant stiffness as seen in Figure 3 and decrease in the soil damping (Figure 4)

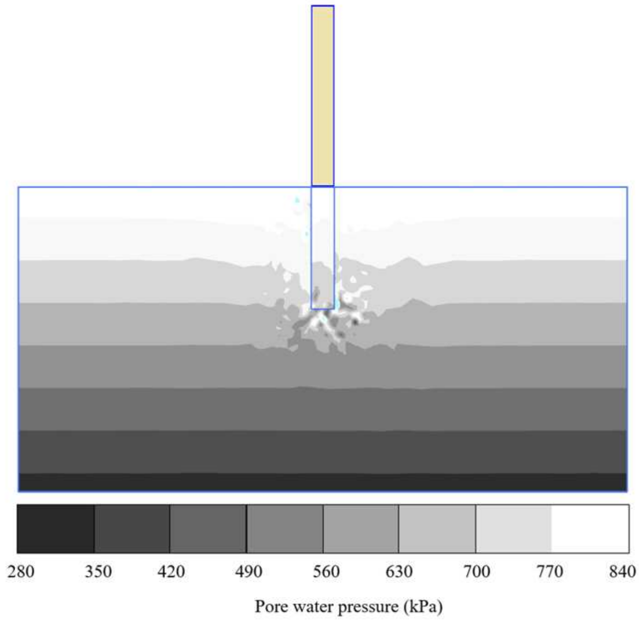

Figure 5. Pore water pressure around the monopile after 100 load cycles with ζ_b = 0.25 (OCR=4.5)

4.2 Normally consolidated clay

4.2.1 Secant stiffness

Figure 6 shows the evolution of the secant stiffness with cycle numbers for monopile in normally consolidated clay. At each loading intensity, the secant stiffness decreases with increasing number of cycles. The stiffness exhibits two trends: a sharp increase during the first N = 2 cycles, which represents the stiffness obtained from the initial loading-unloading curve, followed by a gradual decrease in stiffness as N increases to 100. This phenomenon can be explained by the generation of positive excess pore water pressures which results in a softer response of the monopile. These findings match those reported by Kou et al. (2022) who also observed a decrease of the secant stiffness with the cycle number. The secant stiffness decreases with increasing load magnitudes (ζ_b) owing to an increase in the development of plastic strains around the monopile.

The decrease in secant stiffness can be explained by the generation of positive excess pore water pressures which results in a softer response of the monopile. The softer pile response could have adverse effect on the structural safety of the OWT by causing the natural frequency of the OWT to move towards the 1P rotor frequency which could result in a greater likelihood of resonance.

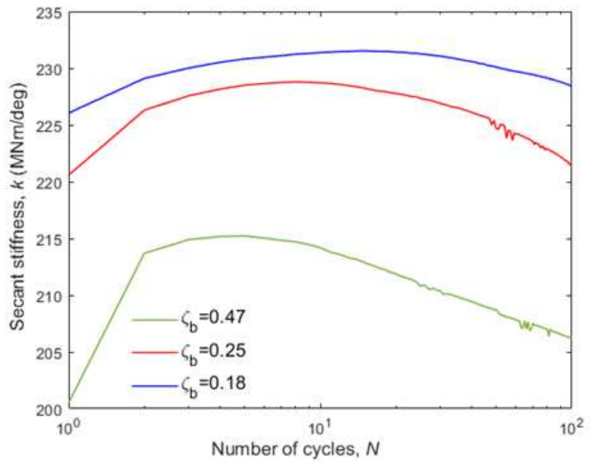

Figure 6. 100 one-way cyclic test results: Evolution of secant stiffness with cycle number (OCR=1.0)

4.2.2 Damping ratio

The evolution of damping with cycle number in normally consolidated clay is shown in Figure 7. As seen in an overconsolidated clay, the damping ratio is higher at greater load intensities. However, in contrast to the overconsolidated clay deposit, after an initial decrease, the damping ratio increases with continuous cyclic loading in a normally consolidated clay. The damping exhibits two trends: a sharp decrease during the first $N = 10$ cycles, which represents the damping obtained from the loop area of the initial loading-unloading curve, followed by a gradual increase as N increases to 100 due to the damping obtained from the loop area of subsequent cycles. This behaviour could be explained by the generation of positive pore water pressures which results in a softer response of the monopile.

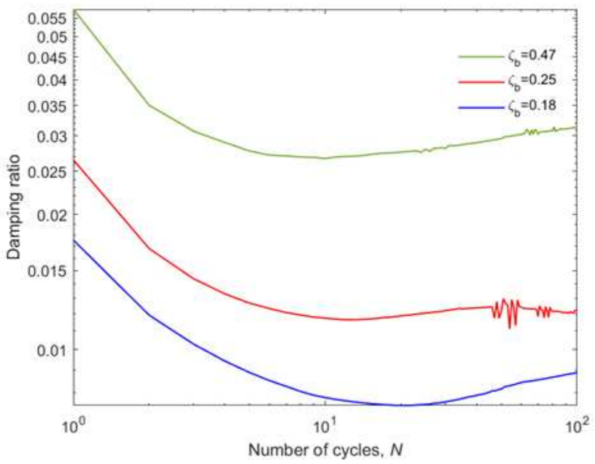

Figure 7. 100 one-way cyclic test results: Evolution of damping with cycle numbers (OCR=1.0)

4.2.3 Pore water pressure

Figure 8 shows pore-water pressure build-up around the monopile during cyclic loading in a normally consolidated clay. Positive excess pore pressure develops on both sides of the monopile, thereby decreasing the effective stress which leads to a decrease in secant stiffness (Figure 6) and an increase in the soil damping (Figure 7).

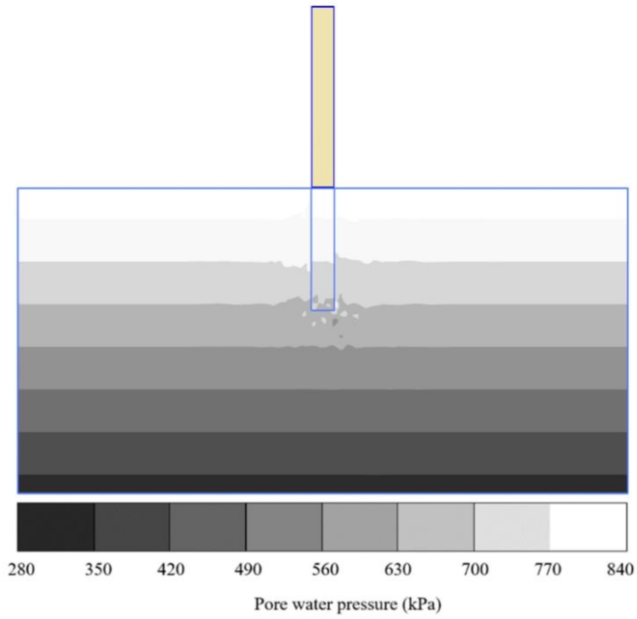

Figure 8. Pore water pressure around the monopile after 100 load cycles with $\zeta_b = 0.25$ (OCR=1.0)

5 CONCLUSION

In this paper, 3D FE analysis was used to investigate the effect of loading intensity and overconsolidation ratio on the evolution of secant stiffness and damping ratio of a monopile installed in a clay deposit subjected to one-way lateral cyclic loading. The monopile showed ratcheting, where rotation accumulates with increasing numbers of load cycles, and the formation of hysteresis loops in each cycle (damping). In normally consolidated clay, the secant stiffness decreased and the damping ratio increased with continuous cyclic loading due to positive excess pore water pressures causing a softer soil response. In contrast, in overconsolidated clay, the stiffness showed an increase (and the damping ratio decreased) because negative excess pressures were generated, leading to higher effective stresses in the soil deposit. The results demonstrate the importance of pore pressure generation in controlling monopile response and provide some guidance in the engineering design of monopiles in clay deposits.

6 ACKNOWLEDGEMENTS

The authors would like to thank the Petroleum Technology Development Fund (PTDF) for funding this research. Support from the EPSRC Collaborative Computational Project in Wave Structure Interaction (CCP–WSI) is also acknowledged (EP/T026782/1).

7 REFERENCES

Abadie, C.N., Byrne, B.W., Houlsby, G.T. 2019. Rigid pile response to cyclic lateral loading: laboratory tests, *Géotechnique* **69**, 863-876.

Beuckelaers, W. 2017. *Numerical modelling of laterally loaded piles for offshore wind turbines*, University of Oxford.

Byrne, B.W., Houlsby, G.T., Burd, H.J., Gavin, K.G., Igoe, D.J., Jardine, R.J., Martin, C.M., McAdam, R.A., Potts, D.M., Taborda, D.M., Zdravković, L. 2020. PISA design model for monopiles for offshore wind turbines: application to a stiff glacial clay till, *Géotechnique* **70**, 1030-1047.

Charlton, T.S., Rouainia, M. 2021. Cyclic performance of a monopile in spatially variable clay using an advanced constitutive model, *Soil Dynamics and Earthquake Engineering* **140**, 106437.

Cheng, X., Wang, T., Zhang, J., Liu, Z., Cheng, W. 2021. Finite element analysis of cyclic lateral responses for large diameter monopiles in clays under different loading patterns, *Computers and Geotechnics* **134**, 104104.

Duque, J., Ochmański, M., Mašín, D., Hong, Y., Wang, L. 2021. On the behavior of monopiles subjected to multiple episodes of cyclic loading and reconsolidation in cohesive soils, *Computers and Geotechnics* **134**, 104049.

Gasparre, A. 2005. *Advanced laboratory characterisation of London Clay*, Imperial College, London.

Gasparre, A., Nishimura, S., Coop, M.R., Jardine, R.J. 2007. The influence of structure on the behaviour of London Clay, *Géotechnique* **57**, 19-31.

Gasparre, A., Coop, M.R. 2008. Quantification of the effects of structure on the compression of a stiff clay, *Canadian Geotechnical Journal* **45**, 1324-1334.

GL, 2005. *Overall damping for piled offshore support structures*. Hamburg, Germany: GL.

Gonzalez, N.A., Rouainia, M., Arroyo, M., Gens, A. 2012. Analysis of tunnel excavation in London Clay incorporating soil structure, *Géotechnique* **62**, 1095-1109.

Hasselman et al. 1973. Measurements of wind-wave growth and swell decay during the joint North Sea wave project (JONSWAP), *Deutschen Hydro-graphischen Institute* 12. Hamburg, Germany.

HM Government, 2019. The Climate Change Act 2008 (2050 Target Amendment) Order 2019. *The National Archives*, London, UK.

Kong, D., Zhu, J., Long, Y., Zhu, B., Yang, Q., Gao, Y., Chen, Y. 2022. Centrifuge modelling on monotonic and cyclic lateral behaviour of monopiles in kaolin clay, *Géotechnique* **72**, 661-674.

Kou, H., Hou, W., Chen, Q., Zhou, N., Zhang, M. 2022. Responses of model monopile to cyclic lateral loadings in clay, *Ocean Engineering* **258**, 111743.

Lai, Y., Li, W., He, B., Wang, L., Xiong, G., Liu, T. 2022. Centrifuge modelling of monotonic and cyclic lateral responses of a hybrid monopile-bucket foundation for offshore wind turbines, *Ocean Engineering* **260**, 111967.

Lai, Y., Wang, L., Hong, Y., He, B., 2020. Centrifuge modeling of the cyclic lateral behavior of large-diameter monopiles in soft clay: Effects of episodic cycling and reconsolidation, *Ocean Engineering* **200**, 107048.

LeBlanc, C., Houlsby, G.T., Byrne, B.W. 2010. Response of stiff piles in sand to long term cyclic lateral loading, *Géotechnique* **60**, 79-90.

Malekjafarian, A., Jalilvand, S., Doherty, P., Igoe, D. 2021. Foundation damping for monopile supported offshore wind turbines: A review, *Marine Structures* **77**, 102937.

Plaxis, B.V. 2022. *PLAXIS 3D 2022 reference manual*, PLAXIS BV, Delft.

Roscoe, K.H., Burland, J.B. 1968. On the generalised stress-strain behaviour of wet clay, *Engineering plasticity* (Eds: Heyman, J. & Leckie, F.A.), 563-609. Cambridge University Press, Cambridge.

Rouainia, M., Muir Wood, D. 2000. A kinematic hardening constitutive model for natural clays with loss of structure, *Géotechnique* **50**, 153-164.

Viggiani, G., Atkinson, J.H. 1995. Stiffness of fine-grained soil at very small strains, *Géotechnique* **45**, 249-265.

Wind Europe, 2020. Offshore wind in Europe: Key trends and statistics 2019. *Technical Report, Wind Europe* **3(2)**, 14–17. Brussels, Belgium.

Xie, M., Lopez-Querol, S. 2021. Numerical simulations of the monotonic and cyclic behaviour of offshore wind turbine monopile foundations in clayey soils, *Journal of Marine Science and Engineering* **9**, 1036.